JOURNAL OF
Materials
CHEMISTRY

Preparation of amorphous magnetite nanoparticles embedded in polyvinyl alcohol using ultrasound radiation

R. Vijaya Kumar,[a] Yu. Koltypin,[a] Y. S. Cohen,[a] Yair Cohen,[a] D. Aurbach,[a] O. Palchik,[a] I. Felner[b] and A. Gedanken*[a]

[a]*Department of Chemistry, Bar-Ilan University, Ramat-Gan 52900, Israel; Fax. +972-3-5351250. E-mail: gedanken@mail.biu.ac.il*
[b]*Racah Institute of Physics, Hebrew University, Jerusalem, Israel*

Received 17th January 2000, Accepted 16th February 2000
Published on the Web 4th April 2000

Uniformly dispersed amorphous nanoparticles of magnetite in polyvinyl alcohol have been obtained by ultrasound radiation. The properties of the as-prepared composite material were characterized by various analytical methods. We have found that the magnetite particles that were 12–20 nm in diameter were very well dispersed in the PVA. The magnetization measurements establish that the composite material is superparamagnetic in nature.

1 Introduction

Nanometre-sized metals, metal oxides and semiconductors are of great interest because they can have physical and chemical properties that are neither characteristic of the atoms nor of their bulk counterparts. The large ratio of surface area to volume can contribute to some of the unique properties of nanoparticles.[1–6] Such nanoparticles are expected to have novel electrical, optical, magnetic, and catalytic properties.[7–11] For example, magnetic nanoparticles can be so small that each particle becomes a single magnetic domain[9] and exhibits unusual phenomena, such as superparamagnetism.[10] Magnetic nanoparticles have been produced in a variety of matrix materials, such as silicon oxides,[12] aluminium oxides,[13] porous glass,[14] vesicles,[15] and different polymers such as poly(styrene),[16] cross-linked poly(styrene) resin,[17] poly(ethylene glycol),[18] poly(methylacrylic acid),[19] poly(4-vinylpyridine),[20] poly(pyrrole),[21] poly(aniline),[22] and poly(vinyl alcohol).[23,24] Ugelstad *et al.*,[25,26] for example, prepared hydrophilic micrometre-sized particles consisting of a polymer latex impregnated with approximately 20% w/w single-domain maghemite. These composite particles were synthesised by the *in situ* oxidation of iron salts within the polymer latex and are commercially available as magnetic carriers. Recently Sohn and Cohen[27] reported the preparation of freestanding copolymer films containing magnetic iron oxide nanoclusters by static casting. The size distribution of the nanoclusters was relatively narrow, and they were uniformly distributed within the films. Magnetic measurements revealed that the nanocomposite films were superparamagnetic. Most recently, Vladimir *et al.*[28,29] reported the preparation of polymer coated magnetite nanoparticles synthesized by 'seed' precipitation polymerization of methylacrylic acid and hydroxyethyl methacrylate in the presence of magnetite nanoparticles. They claimed that the potential use of polymer coated magnetite nanoparticles lies in contrast agents for magnetic resonance imaging (MRI).

Recently, sonochemical processing has proven to be a useful technique for generating novel materials with unusual properties. Sonochemistry arises from acoustic cavitation phenomena, that is, the formation, growth, and implosive collapse of bubbles in a liquid medium.[30] The extremely high temperatures (>5000 K), pressure (>20 MPa), and very high cooling rates ($>10^{10}$ K s^{-1}) attained during cavitation collapse lead to many unique properties in the irradiated solution. Using these extreme conditions, Suslick and his co-workers have prepared amorphous iron[31] by using sonochemical decomposition of metal carbonyls in an alkane solvent. Recently, we have successfully prepared metal polymer composite materials[32a,b] using ultrasound radiation.

In the present investigation we have employed a sonochemical method for the preparation of amorphous magnetite nanoparticles embedded in polyvinyl alcohol. The characterization and properties of the composite material are reported herein.

2 Experimental

A composite material of amorphous magnetite–polyvinyl alcohol was prepared by the sonochemical method. The mixture of iron pentacarbonyl, $Fe(CO)_5$ (1 M, Aldrich) and polyvinyl alcohol (Aldrich, M_w 90000, 99% hydolysed, 1 g) in 100 ml of doubly distilled deoxygenated water was sonicated at 10 °C under an argon flow at 1.5 atm for 3 h with a high intensity ultrasonic probe (Sonics and Materials, VC-600, 20 kHz, 100 W cm^{-2}). The product of the sonication was centrifuged and first washed with deoxygenated water, and then with dry pentane. All of the washings and preparation procedures were performed in an inert glove box ($O_2 < 2$ ppm). The precipitate was dried in vacuum at room temperature overnight.

The XRD measurements were carried out at different temperatures, including room temperature, with a Bruker X-ray diffractometer D8. DSC measurements were carried out on a Mettler DSC 30 by using argon as the carrying gas. Magnetization was measured using a Quantum Design MPMS SQUID magnetometer. The thermogravimetric analysis (TGA) was carried out using a Mettler TGA/STDA 851. The Mössbauer spectroscopy (MS) studies were carried out at 300 K, using a conventional constant acceleration spectrometer. The ^{57}Fe MS were measured with a 50 mCi ^{57}Co : Rh source, and the spectra were least-squares fitted with two sub-spectra. The isomer shift (IS) values are relative to iron metal at 300 K. Transmission electron micrographs were obtained with a JEOL JEM100SX electron microscope. The AFM measurements were carried out in contact mode employing a Topometrix TMX2010 Discoverer using a 7 μm tube scanner and V-shaped tips with a cantilever having a spring constant of 0.032 N m^{-1}. The sample preparation was carried out in the following way. The aqueous solution of the composite material

DOI: 10.1039/b000440p

This journal is © The Royal Society of Chemistry 2000

was spread on a flat mica surface and allowed to dry overnight under vacuum.

3 Results and discussion

Fig. 1 displays the XRD patterns of as-prepared composite material (a), heated at 200 °C for 24 h under high pure nitrogen flow (b), heated at 400 °C for 10 h under high pure nitrogen flow (c), and of untreated commercial polyvinyl alcohol (d). Fig. 1(a) clearly indicates that the as-prepared composite material is amorphous in nature, no trace of a crystalline phase was detected. This correlates very well with the results obtained by Suslick and co-workers,[31] who reported the formation of an amorphous product when a decalin solution of $Fe(CO)_5$ was sonicated under similar conditions. The XRD patterns of the heated composite materials, see in Fig. 1(b),(c), match that of Fe_3O_4, JCPDS card no.: 19-0629. The particle sizes, calculated by using the Debye–Scherer formula,[33] are 20 nm and 30 nm for composite materials heated at 200 °C and 400 °C, respectively.

The topographic AFM images of the polyvinyl alcohol and the as-prepared composite material are depicted in Fig. 2(a) and (b), respectively. Fig. 2(b) shows the topography of the magnetite particles whose sizes vary between 10 nm and 70 nm, protruding from the surface. For comparison we also present the topography of the undoped polymer surface (Fig. 2(a)), which reveals that the adhesion forces for the polymer are also strong and a unified coverage of the flat mica substrate is also observed. The protruding islands observed for the composite particles are missing in the polymer image.

In Fig. 3, we present the TEM pictures of (a) the as-prepared composite material and (b) the composite material heated at 200 °C. Fig. 3(a) clearly shows the excellent dispersion of the Fe_3O_4 particles over the entire area. There is no evidence in this picture of crystallites of Fe_3O_4 particles. The sizes of the Fe_3O_4 particles are 12 and 20 nm for as-prepared materials and for the composite heated at 200 °C, respectively. The sizes are in reasonable agreement with the XRD results.

Fig. 4 shows the DSC curves of (a) polyvinyl alcohol and (b) the as-prepared composite material. The broad endothermic peak detected in Fig. 4(a) at *ca.* 72 °C is attributed to the glass transition temperature; the second endothermic peak at *ca.* 228 °C is attributed to the loss of bonded water; and the third endothermic peak at *ca.* 336 °C is attributed to the structural decomposition of the polyvinyl alcohol. In Fig. 4(b) the broad endothermic peak at *ca.* 58 °C is attributed to the glass transition temperature; the second endothermic peak at *ca.* 226 °C is attributed to loss of bonded water and the third endothermic peak at *ca.* 318 °C is attributed to the structural decomposition of the as-prepared composite material. The reason for the lowering of the glass transition and structural decomposition temperatures could be the existence of the magnetite as an impurity in the as-prepared composite material. We have not observed the amorphous to crystalline transition, the reason for which could be overlapping endothermal peaks of the polyvinyl alcohol indicating the loss of bonded water, and the amorphous-to-crystalline transition which occurs at the same temperature. We have carried out TGA measurements to obtain information on the stability of the polymer and the effect of the magnetite on its stability. Fig. 5 depicts the TGA curves of (a) polyvinyl alcohol and (b) the as-prepared composite material. The pure polymer disintegrates at 340 °C, while the composite material is stable

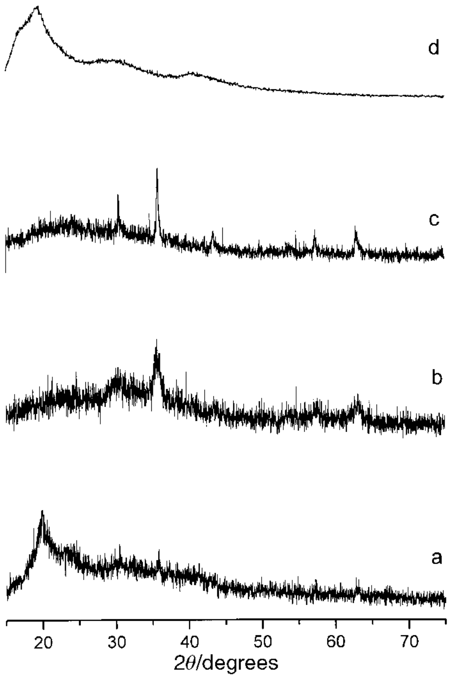

Fig. 1 X-Ray diffraction patters of (a) as-prepared composite material, (b) composite material after heating at 200 °C in high purity N_2 for 24 h, (c) composite material after heating at 400 °C in high purity N_2 for 10 h, and (d) undoped commercial poly(vinyl alcohol).

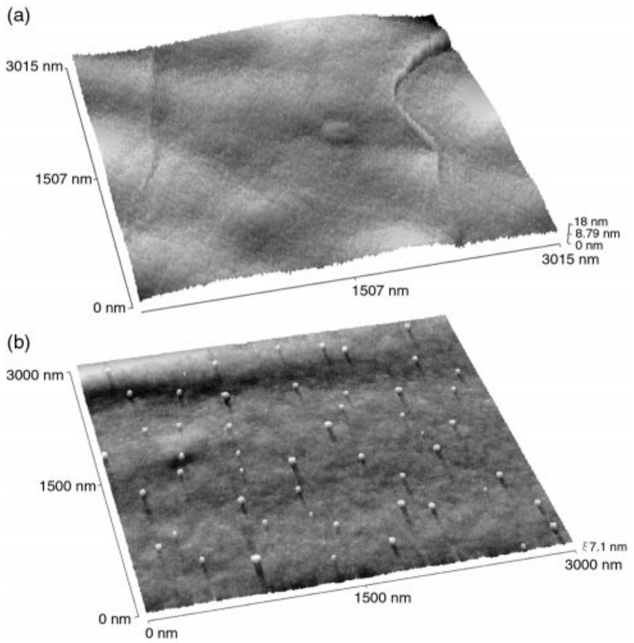

Fig. 2 AFM topographic images of (a) untreated commercial poly(vinyl alcohol), and (b) as-prepared composite material.

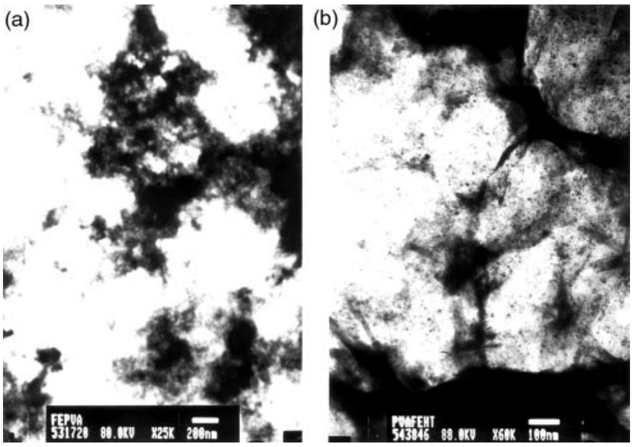

Fig. 3 Transmission electron micrograph pictures of (a) as-prepared composite material, and (b) composite material after heating at 200 °C in high purity N_2 for 24 h.

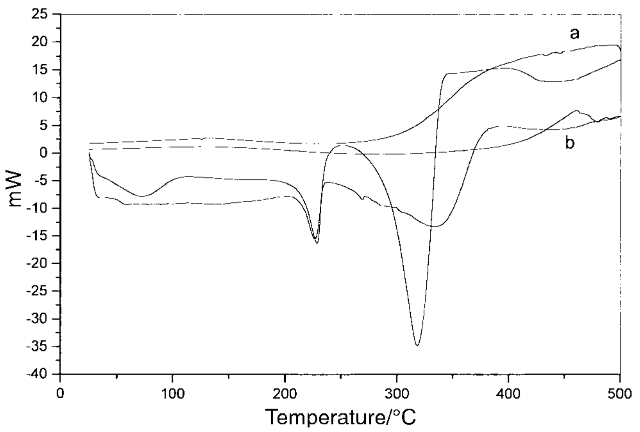

Fig. 4 DSC curves of (a) as-prepared composite material, and (b) undoped commercial poly(vinyl alcohol). The heating rate was 10 °C min^{-1}.

only up to 312 °C. These results are in accordance with the corresponding DSC data. The reason for this could be that the perturbation that the magnetite introduces affects the three-dimensional structure of the polymer. This perturbation weakens the van der Waals interaction between the polymer chains, thus affecting the stability of the polymer, which is reflected in the lowering of the decomposition temperature.

The Mössbauer spectra of the as-prepared composite and the heated composite materials were measured at 300 K and are shown in Fig. 6. For the as-prepared composite material (Fig. 6(a)), the central part of the spectrum exhibits only a broad doublet, which clearly indicates the lack of long-range magnetic ordering. The main information obtained from the experimental spectrum and the computer simulation is the presence of two quadrupole doublets, with a relative ratio of 1 : 2, corresponding to inequivalent Fe sites in the amorphous material. The hyperfine parameters are calculated as: isomer shift $\delta = 0.36$ and 0.41 mm s^{-1} (relative to iron metal), and the quadrupole splitting $\Delta = eqQ/2 = 0.73$ and 1.33 mm s^{-1} with a common line width of 0.43 mm s^{-1}, respectively.

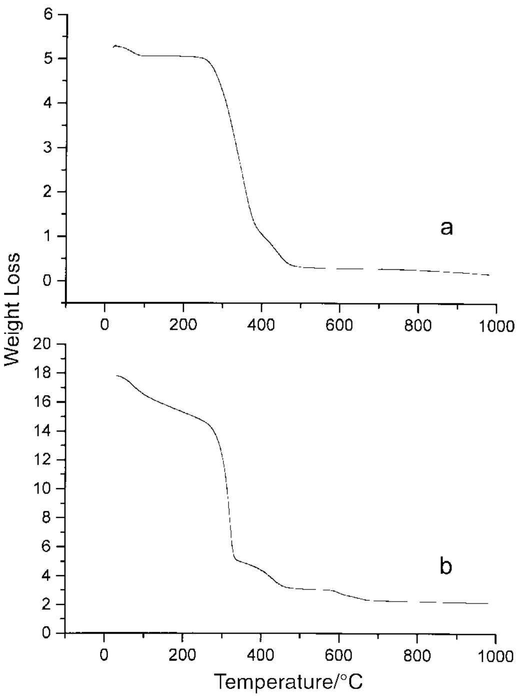

Fig. 5 The TGA curves of (a) undoped commercial poly(vinyl alcohol), and (b) as-prepared composite material. The heating rate was 10 °C min^{-1}.

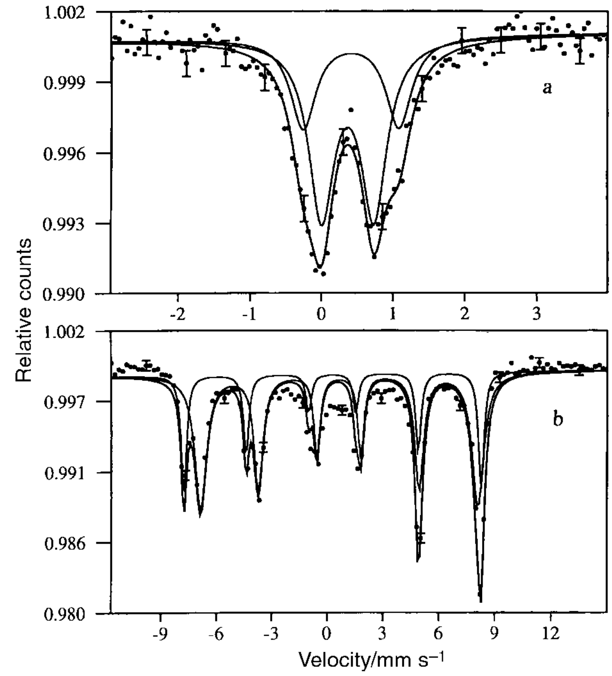

Fig. 6 Room-temperature Mössbauer spectra of (a) as-prepared composite material, and (b) composite material after heating at 200 °C in high purity N_2 for 24 h.

The most important spectrum is that of the as-prepared composite material heated at 200 °C (Fig. 6(b)). This spectrum clearly shows hyperfine magnetic splitting, which is clear evidence for long-range magnetic ordering at room temperature. The interpretation of the spectrum is consistent with the well-established site assignment of Fe_3O_4 (magnetite). In this structure, the Fe^{2+} ions reside in site B, whereas Fe^{3+} ions are distributed over sites A and B. This spectrum was fitted by two sextets: for the sextet attributed to site A (Fe^{3+}), we obtained the hyperfine parameters $H_{\mathrm{eff}} = 497(2)$ kOe and $\delta = 0.29(1)$ mm s^{-1}. For the most intense subspectrum of relative intensity 70(1)% corresponding to site B ($Fe^{3+} + \| Fe^{2+}$), the magnetic hyperfine field is $H_{\mathrm{eff}} = 463(2)$ kOe and $\delta = 0.63$ mm s^{-1}. The common line width is 0.36 mm s^{-1}. The fast electron transfer process (electron hopping) between Fe^{2+} and Fe^{3+} ions produces a completely averaged spectrum for these ions, which do not show a quadrupole effect. The data obtained are in good agreement with the well-known hyperfine parameters of Fe_3O_4,[34] and provide conclusive evidence for the identity of this material as Fe_3O_4.

Fig. 7 shows the magnetization loop of (a) the as-prepared composite and (b) the composite material heated at 200 °C. The

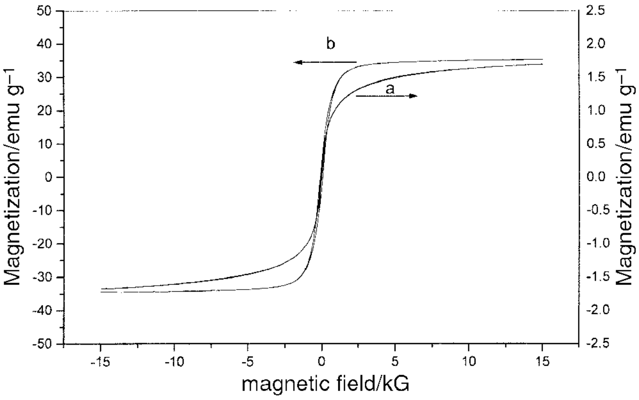

Fig. 7 The room temperature magnetization loop of (a) as-prepared composite material, and (b) composite material after heating at 200 °C in high purity N_2 for 24 h.

magnetization of ferromagnetic materials is very sensitive to the microstructure of any particular sample. If a specimen consists of small particles, its total magnetization decreases with decreasing particle size owing to the increased dispersion in the exchange integral,[35] and finally reaches the superparamagnetic state, when each particle acts as a 'spin' which suppresses the exchange interaction between the particles. A theoretical description of the magnetic behavior of materials consisting of interacting nanopaticles can be found in ref. 36. Thus, we expect to see a dramatic difference between the magnetization of commercial Fe_3O_4 powder and nanocomposite materials. The coercitivity field H_c and magnetization M of (a) the as-prepared composite material at an external magnetic field of 1.5 T are 25 G and 1.65 emu g^{-1} respectively, and for (b) the heated composite material at 200 °C they are 50 G and 35 emu g^{-1}, whereas previously it had been reported[36] that H_c and M for commercial Fe_3O_4 are 293 G and 96.3 emu g^{-1}. It is important to note that we observed no saturation of magnetization as a function of the field, even at 15 kG, for our composite materials. This is further evidence that we are dealing with a superparamagnetic material.

Mechanism for the formation of amorphous Fe_3O_4 nanoparticles embedded in polyvinyl alcohol

The effects of ultrasound radiation on chemical reactions are due to the very high temperatures and pressures which develop during the collapse of a cavity formed in the liquid. There are two regions of sonochemical activity, as postulated by Suslick *et al.*:[37,38] inside the collapsing bubble and the interface between the bubble and the liquid. If the reaction takes place inside the collapsing bubble, as is the case for transition metal carbonyls dissolved in organic solvents, the temperature inside the cavitation bubble can be 5000–2300 K, depending on the vapor pressure of the solvent.[37] On the other hand, if water is used as the solvent, the maximum bubble core temperature that can be reached is close to 4000 K,[39] causing the pyrolysis of water to H and OH radicals. The sonication of $Fe(CO)_5$ in decalin under argon yields amorphous iron[31] while its sonication under air yields amorphous Fe_2O_3.[6] The product obtained is amorphous as a result of the high cooling rates ($>10^{10}$ K s^{-1}) which occurs during the collapse. Following the above mentioned results the sonication of $Fe(CO)_5$ in water–polyvinyl alcohol solution under argon yields amorphous Fe_3O_4 embedded in polyvinyl alcohol. The likely reaction steps are as follows:

$$\mathrm{Fe(CO)_5} \xrightarrow{)))))} \mathrm{Fe} + 5\mathrm{CO} \quad (1)$$

$$\mathrm{H_2O} \xrightarrow{)))))} \mathrm{H^{\cdot}} + \mathrm{OH^{\cdot}} \quad (2)$$

$$\mathrm{H^{\cdot}} + \mathrm{H^{\cdot}} \rightarrow \mathrm{H_2} \quad (3)$$

$$\mathrm{OH^{\cdot}} + \mathrm{OH^{\cdot}} \rightarrow \mathrm{H_2O_2} \quad (4)$$

$$2\mathrm{Fe} + \mathrm{H_2O_2} \rightarrow 2\mathrm{Fe^{2+}} + 2\mathrm{OH^-} \quad (5)$$

$$2\mathrm{Fe^{2+}} + \mathrm{H_2O_2} \rightarrow 2\mathrm{Fe^{3+}} + 2\mathrm{OH^-} \quad (6)$$

Reactions (1), (2), (3), and (4) occur inside the collapsing bubble while reactions (5) and (6) take place in the interfacial region.

4 Conclusions

Uniformly dispersed amorphous nanoparticles of magnetite in a polyvinyl alcohol matrix have been obtained by ultrasound radiation. The magnetic properties of this composite material establish that the composite material is superparamagnetic in nature.

Acknowledgements

Dr. Vijaya Kumar Rangari thanks the Bar-Ilan Research Authority for his post-doctoral fellowship. Prof. A. Gedanken thanks the German Ministry of Science through the Deutsche–Israel Program, DIP, for its support and gratefully acknowledges receipt of a NEDO International Joint Research Grant. Prof. I. Felner and Prof. A. Gedanken thank also the Ministry of Science for an Infrastructure grant. Dr. Yu. Koltypin thanks the Ministry of Absorption, the Center for Absorption in Sciences, for its financial support. The authors are grateful to Prof. M. Deutsch, Department of Physics, and Prof. Z. Malik, Department of Life Sciences, for extending their facilities to us. We thank Prof. Y. Yeshurun for making available for this study the facilities of the National Center for Magnetic Measurements at the Department of Physics, Bar-Ilan University. We also thank Dr. Shifra Hochberg for editorial assistance.

References

1 M. D. Morse, *Chem. Rev.*, 1986, **86**, 1049.
2 W. P. Halperin, *Rev. Mod. Phys.*, 1986, **58**, 533.
3 A. Henglein, *Chem. Rev.*, 1989, **89**, 1861.
4 G. D. Stucky and J. E. MacDougall, *Science*, 1990, **247**, 669.
5 V. V. Kresin, *Phys. Rep.*, 1992, **220**, 1.
6 X. Cao, Y. Koltypin, R. Prozorov, G. Katabi and A. Gedanken, *J. Mater. Chem.*, 1997, **7**, 2447.
7 F. Hache, D. Richard and C. Flytzanis, *J. Opt. Soc. Am. B*, 1986, **3**, 1647.
8 S. Kirkpatrick, *Rev. Mod. Phys.*, 1973, **45**, 574.
9 C. Kittel, *Phys. Rev.*, 1946, **70**, 965.
10 C. P. Bean and J. D. Livingston, *J. Appl. Phys.*, 1959, **30**, 120.
11 A. Henglein, *Chem. Rev.*, 1986, **89**, 1861.
12 R. D. Shull, J. J. Ritter and L. J. Swartzendruder, *J. Appl. Phys.*, 1991, **69**, 5414.
13 A. Gavrin and C. L. Chien, *J. Appl. Phys.*, 1990, **67**, 938.
14 N. F. Borelli, D. L. Morse and J. W. H. Schreurs, *J. Appl. Phys.*, 1983, **54**, 3344.
15 S. Mann and J. P. Hannington, *J. Colloid Interface Sci.*, 1988, **22**, 326.
16 M. Senna and J. Lee, *Colloid Polym. Sci.*, 1975, **76**, 273.
17 R. F. Ziolo, E. P. Giannelis, B. A. Weinstein, M. P. O'Horo, B. N. Ganguly, V. Mehrotra, M. W. Russell and D. R. Haffman, *Science*, 1992, **257**, 219.
18 B. E. Van Beers, J. Pringot and B. Gallez, *J. Radiol.*, 1995, **76**, 991.
19 G. D. Mendenhall, Y. Geng and J. Hawang, *J. Colloid Interface Sci.*, 1996, **184**, 519.
20 L. Chen, W. J. Yang and C. Z. Yang, *J. Mater. Sci.*, 1997, **32**, 3571.
21 M. D. Butterworth, S. A. Bell, S. P. Armes and A. W. Simpson, *J.Colloid Interface Sci*, 1996, **183**, 91.
22 M. Kryszewski and J. K. Jeszka, *Synth. Met.*, 1998, **94**, 99.
23 A. E. Varfolomeev, D. Yu. Godovskii, G. A. Kapustin, A. V. Volkov and M. A. Moskvina, *JETP Lett*, 1998, **67**, 39.
24 J. Lee, T. Isobe and M. Senna, *J. Colloid Interface Sci.*, 1996, **177**, 490.
25 K. S. Nustad, T. E. Funderud, A. Berge and J. Ugelstad, in *Scientific Methods for the Study of Polymer Colloids and their Applications*, ed. F. Candau and R. H. Ottewill, 1990, Kluwer Academic, Dordrecht, p. 517.
26 J. Ugelstad, P. Stenstad, L. Kilaas, W. S. Prestvik, P. Herje, A. Berge and E. Hornes, *Blood Purification*, 1993, **11**, 349.
27 B. H. Sohn and R. E. Cohen, *Chem. Mater.*, 1997, **9**, 264.
28 S. Z. Vladimir, D. S. Filimonov, I. A. Presnyakov, R. J. Gambino and B. Chu, *J. Colloid Interface Sci.*, 1999, **49**, 212.
29 P. A. Dresco, S. Z. Vladimir, R. J. Gambino and B. Chu, *Langmuir*, 1999, **15**, 1945.
30 K. S. Suslick (editor), *Ultrasounds: its Chemical, Physical and Biological Effects*, VCH, Weinheim, 1988.
31 K. S. Suslick, S. B. Choe, A. A. Cichowals and M. W. Grinstaff, *Nature*, 1991, **353**, 414.
32 (*a*) S. Wizel, R. Prozorov, Y. Cohen, D. Aurbach. S. Margel and A. Gedanken, *J. Mater. Res.*, 1998, **211**, 13; (*b*) S. Wizel, S. Margel, T. C. Rojas, A. Fernandez, R. Prozorv and A. Gedanken, *J. Mater. Res.*, 1999, **14**, 3913.
33 H. Klug and L. Alexander, *X-ray Diffraction procedures*, Wiley, New York, 1962, p. 125.

34 N. N. Greenwood and T. C. Gibb, *Mössbauer Spectroscopy*, Chapman and Hall, London, 1971, p. 251.

35 S. R. Elliott, *Physics of Amorphous Materials*, Longman, London and New York, 1984, p. 350.

36 X. Cao, Yu. Koltypin, G. Katabi, R. Prozorov, I. Felner and A. Gedanken, *J. Mater. Chem.*, 1997, **7**, 1007.

37 W. B. McNamara III, Y. T. Didenko and K. S. Suslick, *Nature*, 1999, **401**, 772.

38 K. S. Suslick, D. A. Hammerton and R. E. Cline, *J. Am. Chem. Soc.*, 1986, **108**, 5641; M. W. Grinstaff, A. A. Cichowlas, S. B. Choe and K. S. Suslick, *Ultrasonics*, 1992, **30**, 168.

39 V. Misik, N. Miyoshi and P. Riesz, *J. Phys. Chem.*, 1995, **99**, 3605.